Eur. Phys. J. D **31**, 53–61 (2004)
DOI: 10.1140/epjd/e2004-00115-2

THE EUROPEAN PHYSICAL JOURNAL D

Ag–Co clusters deposition on Ag(100): an atomic scale study

A. Dzhurakhalov[1,2], A. Rasulov[1,3], T. Van Hoof[1], and M. Hou[1,a]

[1] Physique des Solides Irradiés et des Nanostructures CP234, Université Libre de Bruxelles, boulevard du Triomphe, 1050 Brussels, Belgium
[2] Theoretical Dept., Arifov Institute of Electronics, F. Khodjaev Str. 33, 700125 Tashkent, Uzbekistan
[3] Ferghana Polytechnic Institute, Ferghana Str. 86, 712022 Ferghana, Uzbekistan

Received 27 April 2004 / Received in final form 11 June 2004
Published online 31 August 2004 –

Abstract. The slowing down of $Co_{10}Ag_{191}$ and $Co_{285}Ag_{301}$ nanoclusters on a Ag (100) surface is studied at the atomic scale by means of classical Molecular Dynamics simulations. The slowing down energy, 0.25 to 1.5 eV/atom, is characteristic of low energy cluster beam deposition and aerosol focused beam techniques. The two clusters differentiate by their size, stoechiometry and structure. While Co forms one or several groups just beneath the cluster surface in $Co_{10}Ag_{191}$, $Co_{285}Ag_{301}$ displays a core-shell structure where Ag forms one complete monolayer around the Co core. As a consequence of the impact, the smallest cluster undergoes deep reorganization and becomes fully epitaxial with the substrate. The larger one only undergoes partial accommodation and partially retains the memory of its initial morphology. For both, after impact, the Co forms one group covered by Ag. The substrate damage is significant and depends on the slowing down energy. It results in a Ag step surrounding the cluster which may be more than one atomic layers high and isolated add-atoms or small monolayer islands apart from the step. The latter originate from the cluster and the former from the substrate. Further details in the consequences of the impact are given, concerning the cluster penetration, its deformation and lattice distortions, with emphasis on the cluster size and stoechiometry.

PACS. 35.40.-c – 61.46.+w Nanoscale materials: clusters, nanoparticles, nanotubes, and nanocrystals – 07.05.Tp Computer modeling and simulation

1 Introduction

Nanoclusters on surfaces are interesting for a wide range of chemical, magnetic, electronic and optical properties. Bimetallic particles can be produced displaying either core-shell structures [1–3] or forming alloys with, eventually, a segregated surface [4,5]. The possibilities of synthesis outside equilibrium conditions widely increase the range of possible cluster composition and structure [6,7]. Such particles can be modelled at the atomic scale [8–11] allowing detailed comparison with experiment. Such studies are facilitated either by depositing the clusters on surface or embedding them into a matrix. Deposited and embedded particles can be modelled on their turn, at the atomic scale [12–16]. By accumulating them, it is possible to synthesized nanostructured layers with specific properties. Cluster assembled films are formed by deposition on a surface [17] and such films could be modelled as well [18–21]. Specifically, clusters on surfaces can be obtained by atomic deposition followed by thermal diffusion. This method applies for atomic species forming islands rather then wetting the surface. Such a method was used, for instance, to produce cobalt clusters on a silver surface [22]. These clusters precipitate preferentially on pre-existing defects, or the atoms form defects at landing, themselves acting as sinks for cluster growth. Clusters in the gas phase are produced by laser ablation [23] or by condensation [24] and then extracted into a supersonic beam directed toward the substrate surface. By the latter method, clusters at thermodynamic equilibrium are formed while clusters outside equilibrium can be synthesized with the former. These both techniques allow mass selection so that homogeneous populations of deposited clusters can be formed, with identical deposition conditions. It is well-known from both experiment [23] and modelling [14] that clusters slowing down at supersonic velocities do not fragment upon impact. Whether they remain intact or undergo restructuring upon impact is still an open issue which merits attention. In particular, the question to know to which extent clusters retain their original characteristics needs an answer when the clusters are considered as possible building blocks for transferring their specific properties to the macroscopic scale.

In the present paper, this question will not be addressed as a whole. The case of noble elemental clusters

[a] e-mail: mhou@ulb.ac.be

Table 1. Physical quantities used to estimate the characteristic electron-phonon coupling time in Ag.

Debye temperature (K)	Conduction electronic density (m^{-3})	Thermal conductivity (W/m.K)	Fermi energy (J)	Atomic mass (kg)	Coupling time (ps)
215.0	$5.86e^{28}$	418.0	$0.8796e^{-18}$	$1.791e^{-25}$	22.557

deposited on a crystalline substrate having the same elemental nature was the purpose of previous studies [14,20,21]. The case of metallic alloy clusters and nanostructured films formed by their accumulation was discussed in [16,21,25]. The present study focuses on bimetallic clusters formed by non-miscible elements. Such clusters can be synthesized outside thermodynamic equilibrium. The case of the Co–Ag system is selected, as it has already been the subject of several experimental [26–29] and modelling [12,30] studies. Truncated octahedral Co_xAg_{201-x} isolated clusters, with $0 \leq x \leq 201$ were already studied by means of a Metropolis Monte Carlo method [11]. They have an fcc structure and 201 is the smallest number of atoms with which an ideal compact truncated octahedron can be constructed. The spatial distribution of Co and Ag in this cluster was shown to be the consequence of a balance between Ag position relaxation and Co binding. This balance is temperature dependent. When the amount of Ag is sufficient, it systematically forms a layer around a Co core. However, when Co atoms are only a few (no more than 10), they are located just beneath the cluster surface, either as one oblate group beneath a facet, or as subgroups of no more than 5 atoms beneath a vertex.

The slowing down of such a cluster, with $x = 10$, is here studied in detail in comparison with a bigger one, $Co_{285}Ag_{301}$. This latter cluster is also an ideal truncated octahedron and it has a core-shell structure. The stoechiometry is such that the core is pure Co and the shell is made of one monolayer of Ag. The substrate Ag surface has {100} orientation and the slowing down occurs at room temperature.

These two clusters undergo different transformations upon impact, related to their different size and structure and it is the purpose of the present paper to identify the consequences of the impact on these transformations.

Section 2 briefly describes the Molecular Dynamics (MD) model employed and the slowing down conditions. The detailed study of the cluster slowing down is presented in Section 3 where a distinction is made between a statistical analysis over several slowing down histories and an analysis cluster by cluster. An overall picture of the slowing down and related cluster modifications emerges, which is summarised in Section 4.

2 The model

The MD model employed is already described elsewhere [20] and will only be briefly summarised. The equations of motion of the atoms in the system are integrated stepwise in time with the algorithm in [31]. Forces are derived from an Embedded Atom Model potential (EAM) proposed in [32] and account, in addition, for a contribution of electron-phonon coupling. This is done by means of a friction term which governs the exchange of energy between the ionic and the electronic systems, assuming a constant electronic temperature. It is shown in [20] how an approximate model can be established to evaluate the strength of the coupling with no adjustable parameters. The physical quantities needed are known from experiment in the case of pure elements, and it is assumed that the electronic density at the Fermi level is one electron per atom. The electron-phonon coupling contributes to dissipate the energy brought by the cluster in the impact and enhances the local cooling of the system. As compared to elemental systems, more complexity occurs in the present case as we have to deal with two different metallic elements that are not homogeneously distributed. The approximated electron-phonon coupling model employed is unsuitable to correctly describe the transport of heat by the electronic system through an interface between two elemental subsystems as in a core-shell structured cluster. It is considered here that, since the substrate is pure silver, it will be sufficient to model the electron-phonon coupling for pure silver and to neglect the difference with cobalt. The physical quantities used to estimate the electron-phonon coupling in Ag, and the characteristic coupling time deduced at room electronic temperature are given in Table 1.

The major parameter which governs the interatomic interactions in the system is, of course, the potential. Its assessment for the Co–Ag system is thoroughly discussed in [10,12] and this discussion will not be repeated. This potential was used to discuss the equilibrium properties of Co clusters embedded in Ag and Co–Ag free clusters. The difference with the present case is the impact of the clusters on a surface, involving energies up to 1.5 eV per atom, which is much higher than those involved at thermal equilibrium. However, at this energy, the shortest Ag–Ag separation distance involved in the simulations presented below is 2.124 Å at 1.5 eV/at. It is similar for Co–Co and Ag–Co pairs at the same energy. Such distances are still of the order of the first neighbour distance for which the EAM potential is designed.

In order to evaluate the modification of the clusters as a result of their impact on a Ag substrate surface, a set of characterisation functions is used.

A structure factor is used to measure the epitaxial accommodation of the clusters with the substrate. It is measured inside the cluster and gives information about the periodicity in one direction

$$S = \frac{1}{N} \sum_{j=1}^{N} e^{i\mathbf{k}\mathbf{r}_j}. \quad (1)$$

In this expression, $\mathbf{k}$ is the wave vector, $\mathbf{r}_j$ is the position of the atom j and N is the total number of atoms in the cluster. If the periodicity in the direction of $\mathbf{k}$ corresponds to the inverse of $|\mathbf{k}|$, then the value of $|S|^2$ is unity. If there is no such periodicity in this direction, $|S|^2$ is zero. In order to measure the epitaxial accommodation of the deposited cluster with the substrate, substrate lattice wave vectors are used

$$\mathbf{k} = \frac{4\pi}{a_0}(h, k, l) \tag{2}$$

where a_0 is the substrate lattice parameter, and h, k and l are Miller indices of lattice directions.

A pair correlation function is used to characterise short-range order in the clusters,

$$g(r) = \frac{1}{2(N-1)} \sum_{i=1}^{N-1} \sum_{j=i+1}^{N} \delta(r_{ij} - r) \tag{3}$$

where δ is the Dirac function, N is the number of atoms in the cluster and r_{ij} the distance between atoms i and j in the cluster. The pair correlation function gives the number of atomic pairs separated by a given distance, r. This function is calculated separately for the different kinds of pairs: Co–Co, Ag–Ag and Ag–Co. It is characteristic of the lattice structure.

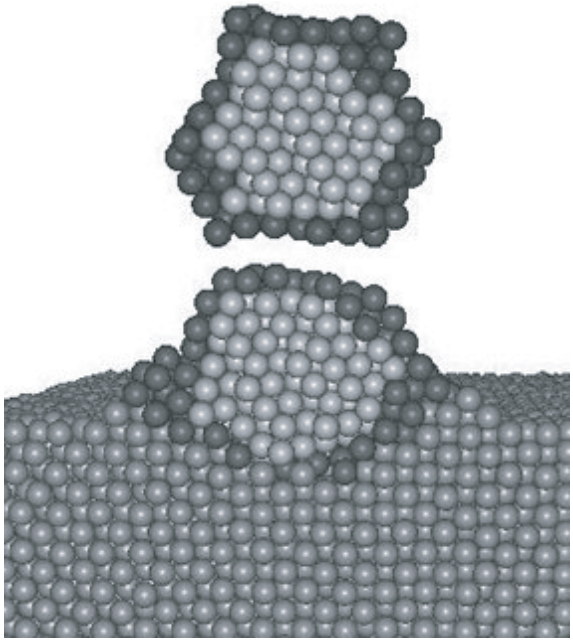

Fig. 1. Initial and final configuration of a $Co_{285}Ag_{301}$ cluster slowing down at 0.5 eV/atom kinetic energy. The Ag cluster atoms are in dark, the substrate atoms in medium grey and the Co atoms in light grey.

3 Cluster slowing down

If one defines the impact characteristic time as the time needed for the cluster to convert its centre of mass kinetic energy into potential energy, and this potential energy to convert into kinetic energy into the whole system, it can be estimated as of the order of 5 ps, which is smaller than the electron-phonon coupling time at room temperature (20 ps). The slowing down of a cluster is followed during 150 ps in order to track possible thermally activated processes. At the end of these 150 ps MD evolution, particle trajectories are fully decorrelated from the initial trajectories and the system is in a thermal equilibrium state which may be metastable. Whether this state has a sufficiently long lifetime to be observed is not known and this question needs comparison with experiment to be settled. However, if an incident cluster undergoes modifications because of the impact, the probability to retrieve its initial state once deposited is vanishingly small. These modifications may thus be considered as permanent, whatever further thermally activated modifications are still possible.

The discussion of the slowing down of the clusters on a Ag (100) surface will be split into two parts. The first one focuses on statistical aspects and the second one to individual aspects, where the sensitivity of the final state of the cluster on the slowing down conditions is examined.

3.1 Statistical approach

In order to mimic a uniform collimated beam, the slowing down, always at normal incidence, is repeated ten times with the same cluster with a given initial kinetic energy, selecting the impact points on the surface and its orientations with respect to the surface at random. Each impact is followed during 150 ps at room temperature. Within the 150 ps evolution time considered, thermally stimulated configuration modifications may have a sufficiently high probability to take place. The slowing down is characterised by several significant features. These can be illustrated with the help of Figure 1 which represents a cut in the cluster before its deposition and in the cluster-substrate system after 150 ps evolution. The $Co_{285}Ag_{301}$ cluster is represented and the slowing down energy is 0.5 eV/atom. The final system is characterised by a limited penetration of the cluster into the substrate. It undergoes some deformation accompanied by structural accommodation of the cluster with the substrate, which is limited in the case of Figure 1. At the same time, the upper part of the cluster may retain its initial atomic arrangement. It the case of Figure 1, some damage is created in the substrate and the Ag cluster shell tends to spread on the substrate surface. While the Co core is only moderately affected by the slowing down, the Ag lattice, which is already distorted initially, undergoes further deformation as a consequence of the impact. All these characteristics of course depend on the incident energy as well as on the cluster size, composition and energy. We now turn to their systematic study for $Co_{285}Ag_{301}$ and $Co_{10}Ag_{191}$.

The first characteristic of the slowing down in the energy range considered is the penetration of the clusters into the substrate and the related damage. Surface damage production induced by the soft landing of Co atoms was already studied, both experimentally and by MD in [30] and

surface tunnelling microscopy showed it to be significant. The situation may be different if the incident Co atoms are bound inside clusters as in the present case. At the low energies considered (no more than 1.5 eV per atom), the cluster penetration, if any, is only partial. Co is always found regrouped into one cluster surrounded by a layer of silver. When it penetrates, the cluster displaces Ag atoms from the substrate with the consequence of the formation of add-atoms. For both clusters, the fraction of cluster atoms with final positions below the substrate surface is the same and is close to linearly increasing with the slowing down energy. It is close to 3 percent at 0.25 eV/at and 30 percent at 1.5 eV/at. According to a rule of volume conservation, in the case of the smallest cluster, the number of substrate atoms displaced above the surface is exactly equal to the number of cluster atoms below this surface. It is somewhat smaller for the larger cluster since the volume per Co atoms below the surface is less than the volume per Ag atoms in the substrate. Figure 2 shows the maximal penetration depth of the incident clusters (Fig. 2a) and the height of the layer formed by substrate atoms above the surface (Fig. 2b) as functions of the incident energy. The distinction is made between the penetration of each of the elements forming the incident clusters. The results are averaged over ten independent slowing downs at each energy and the standard errors on the mean are given. Not surprisingly, the maximal penetration is a monotonically increasing function of the incident energy and it is limited to 4 atomic layers for the largest cluster. The smallest cluster does not penetrate two layers, in the average, at the highest energy considered. The largest cluster systematically penetrates deeper than the smallest one. Systematically as well, Co, initially surrounded by Ag atoms has less penetration than Ag and still remains surrounded by its silver shell. Except for the smallest cluster with incident energy lower than 0.5 eV/at, Co and Ag atoms are always found at least one layer deep in the substrate. This suggests that, in real experiments, substrate damage would be particularly difficult to avoid.

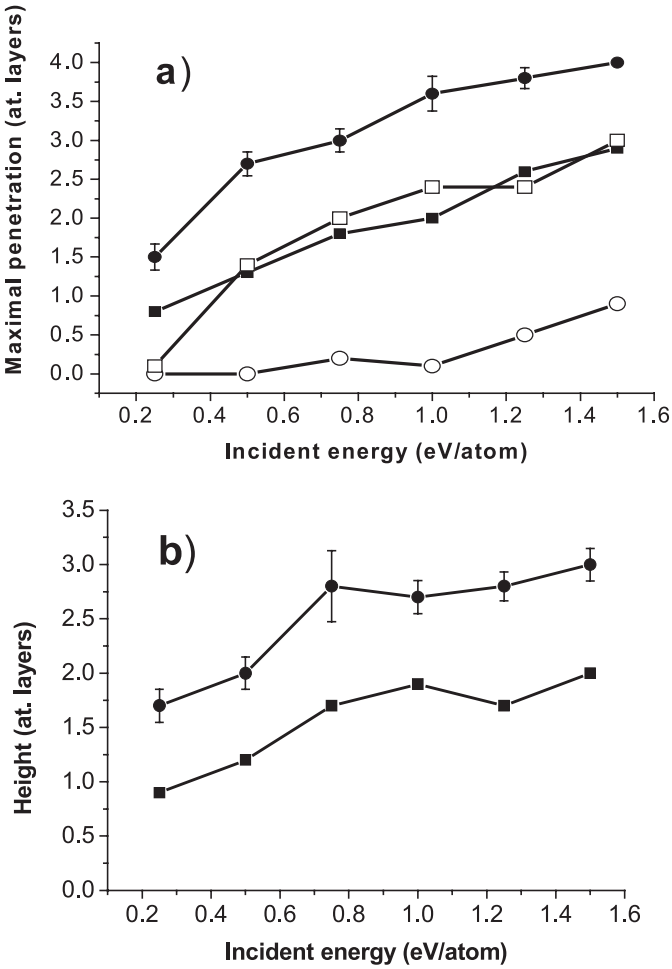

Fig. 2. Maximal penetration (a) and mean height of the step around the clusters (b) as functions of the slowing down energy. In Figure 2a, dark squares represent the results for Ag in the small cluster, dark circles for Ag in the big clusters, open circles for Co in the small clusters and open squares for Co in the big clusters. In Figure 2b, circles provide the results for the small cluster, squares for the big clusters. The error bars displayed represent the standard error on the mean and are only shown for one curve per plot. They are similar for the other curves.

As a consequence of the impact, Ag atoms leave the cluster and form add-atoms. Add-atoms are either found regrouped and forming a step at the periphery of the cluster, or they are found isolated at larger distances from the cluster. The latter, in their large majority, are found to originate from the cluster itself while the former are substrate atoms displaced during the penetration of the cluster. Part of the induced damage can be appreciated in Figure 2b where it is shown that displaced Ag atoms form layers around the cluster which height, in the average, is also an increasing function of the incident energy. Figure 3 illustrates the second contribution to surface damage. It shows, as a function of the impact energy, the mean fraction of Ag atoms, originated from the cluster and found as isolated add-atoms or isolated add-atoms groups at the end of the simulation. An add-atom is considered as isolated if no other add atom is present in its first neighbourhood. An isolated add-atom group is a group of first neighbouring add-atoms. Each of them is at a distance from the step around the cluster larger than a first neighbour distance. This fraction is found increasing with the impact energy in the case of both clusters. It is systematically larger however and its increase with the slowing down energy is the fastest in the case of the biggest cluster. This shows that the kinetic energy of the incident Ag atoms stimulates their diffusion away from the cluster area.

The second characteristic is the deformation of the cluster due its interaction with the substrate surface. This deformation can be estimated by an aspect ratio. If one considers the z-axis perpendicular to the (001) substrate surface and the x and y axes parallel to the [100] and [010] direction respectively, we use, to estimate an aspect ratio, the distance l between the cluster atoms having the highest and the lowest z-coordinate, the distance L_x between cluster atoms with the lowest and highest x-coordinate and L_y similarly. The ratios l/L_x and l/L_y are measured

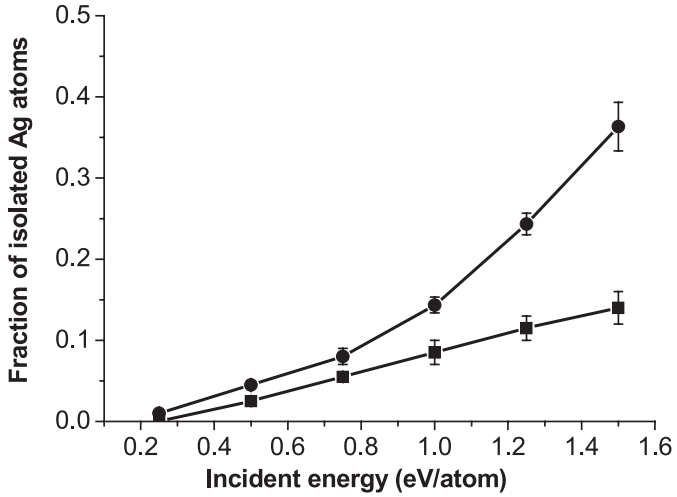

Fig. 3. Fraction of isolated Ag add atoms as relative to the total number of Ag atoms in the clusters, as a function of the slowing down energy. Squares: small cluster, circles: big cluster.

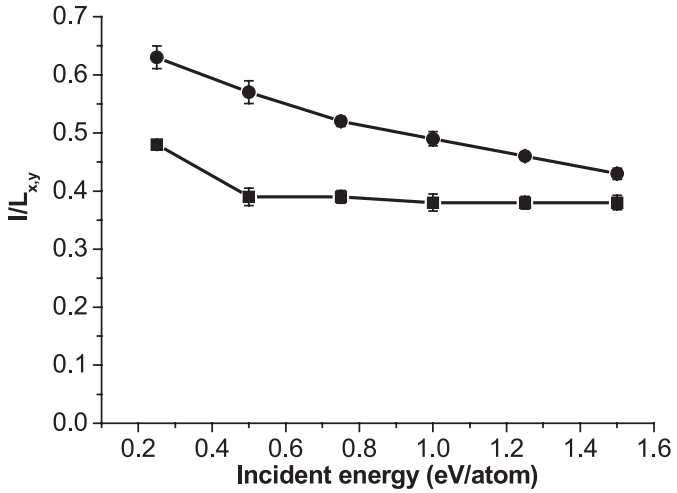

Fig. 4. Aspect ratio of the deposited clusters as a function of the slowing down energy. Results using L_x and L_y are cumulated. Squares: small cluster, circles: big cluster.

and averaged over 10 impacts. Within statistical uncertainty, these ratios are equal and their dependence on the slowing down energy is given in Figure 4 for the two clusters considered. As truncated octahedra, the initial clusters have an aspect ratio close to unity. Their diameters are 1.6 nm and 2.4 nm respectively. The results in Figure 4 show that, as a consequence of the impact, the clusters are strongly deformed, spreading out over the cluster surface. If one excepts the lowest energy considered (0.25 eV/atom) the spreading is not significantly energy dependent for the smaller cluster and only weakly for the largest. Strikingly enough, the biggest cluster undergoes less deformation than the smaller one. This can be explained in terms of binding energy of the free clusters. Indeed, the 0 K binding energy of the smallest cluster (2.503 eV/atom) is smaller than that of the larger one (3.249 eV/atom). The binding energy is an increasing function of the number of atoms in the cluster, and the effect is here reinforced by the fact that the relative concentration of Co is higher in the large cluster, which has a larger binding energy than Ag. Therefore, the deformation of the smallest cluster subsequent to the impact requires less energy per atom and it is larger. Since mean aspect ratios are estimated over 10 statistically independent cases, the associated standard deviations are only three times larger than the standard error on the mean represented in Figure 4. This demonstrates that the dispersion of the results is rather small and thus that, for both kinds of clusters, the aspect ratio is only weakly dependent on the impact point or the incidence cluster orientation.

A third characteristic is the structural accommodation of the clusters with the surface substrate. This one is measured by means of the structure factor defined above and measured for the cluster atoms only. Typical time evolutions of the structure factor are given in Figure 5. In this figure, the **k**-vector used is $(0, 0, 4\pi/a)$, pointing toward the substrate surface normal. In order to provide general trends, the time dependencies of the structure factor are given for all impacts, for both clusters at the lowest and the highest energies considered in this work. Only the results for the contribution of Ag atoms are shown in Figure 5. In the case of the small cluster, the epitaxial accommodation is quite efficient. The distribution of the final $|S|^2$-values is narrow and somewhat lower than unity, because of thermal vibrations and lattice distortions caused by the presence of some Co atoms in the cluster. In contrast, the final values obtained for the larger cluster are lower and more widespread. This is a consequence of the larger distortion caused by the larger fraction of Co in the cluster, and of a more limited epitaxial accommodation due to the larger cluster size. Mean final values are insensitive to the impact energy of the small cluster, epitaxy being reached anyway. For the larger cluster, the mean structure factor value is somewhat higher at the highest energy, showing, as already found in other systems [16], that the impact energy helps enhancing epitaxial accommodation. Figure 5 also provides information about the cluster accommodation evolution. In Figures 5a, 5b and 5d, for most cases, the evolution is terminated after 30 ps. This is however not always the case, as pointed for one cluster in Figure 5a where a jump of the structure factor is identified, which is the signature a thermally activated process. Similar events were found in other cases not represented in Figure 5. The time of one impact, as defined above, is no longer than 5 ps. The typical evolution time is close to one order of magnitude larger (30 ps) and, therefore, the cluster modifications cannot be assigned to the impact. This conclusion is supported by a detailed analysis of Figures 5a, 5b and 5d showing that the structure factor keeps close to zero during the time of the impact. It can be at least partially assigned to the local heating since the characteristic electron-phonon coupling time is 20 ps at room temperature in the present model. One thus has to conclude that the process of epitaxial accommodation starts after the impact is terminated and the combined effect of local heating and the substrate temperature is responsible

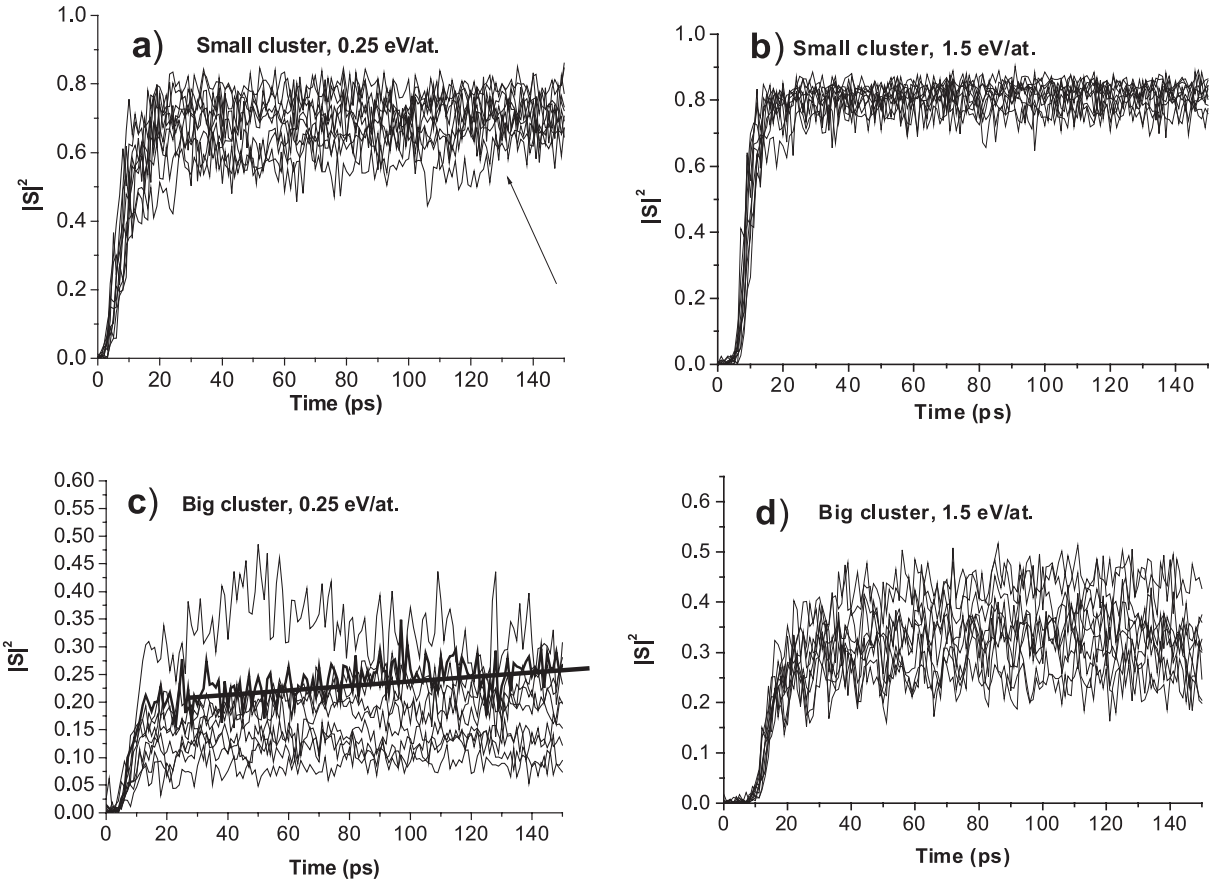

Fig. 5. Structure factor as a function of time during the slowing down. (a) Ten small cluster slowing downs at 0.25 eV/atom, (b) ten small cluster slowing downs at 1.5 eV/atom, (c) ten big cluster slowing downs at 0.25 eV/atom, (d) ten big cluster slowing downs at 1.5 eV/atom. In (a), the arrow shows the occurrence of a thermally activated increase of the structure factor. In (c), one evolution is emphasised and a regression line, plotted to guide the eyes, shows the corresponding regular increase of the structure factor with time.

for the epitaxial accommodation. The case of Figure 5c is different. This figure shows that, for the larger cluster, at low impact energy, the epitaxial accommodation is a still slower process. As shown by a regression line drawn for one of the clusters, the evolution is not always terminated after 150 ps. In this case, the impact energy (0.25 eV/atom) produces less damage in the cluster than at 1.5 eV/atom (Fig. 5d), so that the energy barrier to surmount for reaching epitaxial accommodation is higher. This energy barrier is probably to a large extent the energy required to rotate the Co group toward epitaxial correspondence with the substrate orientation.

A fourth characteristic of the slowing down is the morphological accommodation of the cluster with the substrate. This accommodation is not conveniently described by one single parameter. In the many impacts investigated, the main morphological features observed are a re-faceting of clusters and an interfacial alignment with ⟨100⟩ and ⟨110⟩ substrate surface directions. By systematic 3-dimensional visualisation of the slowing down of the clusters, it is found that the small cluster truncated octahedral morphology is indeed fully destroyed by the impact at all energies investigated. Simultaneously to the epitaxial accommodation with the substrate, new facets are formed with {111} and {100} orientations. One typical example is shown in Figure 6. The facets induce alignment with either ⟨110⟩ or ⟨100⟩ surface directions, leading to a markedly polygonal cluster-substrate interface, often, as shown in Figure 6, in the form of a octahedron

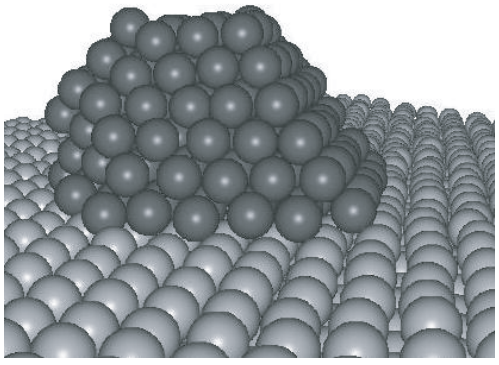

Fig. 6. $Co_{10}Ag_{191}$ cluster after deposition at 0.25 eV/atom. The cluster was initially an truncated octahedron and transformed upon impact into a half octahedron truncated on top.

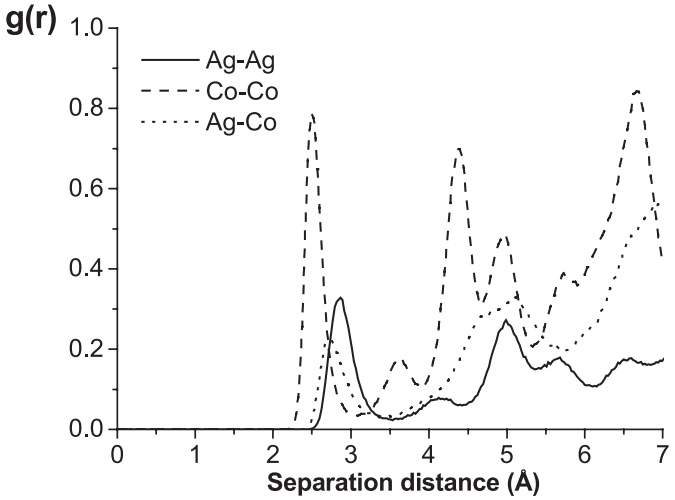

Fig. 7. Pair correlation functions measured in the $Co_{285}Ag_{301}$ cluster after slowing down with 1.5 eV/atom incident energy. Solid line: Ag–Ag pairs, dashed line: Co–Co pairs, dotted line: Ag–Co pairs.

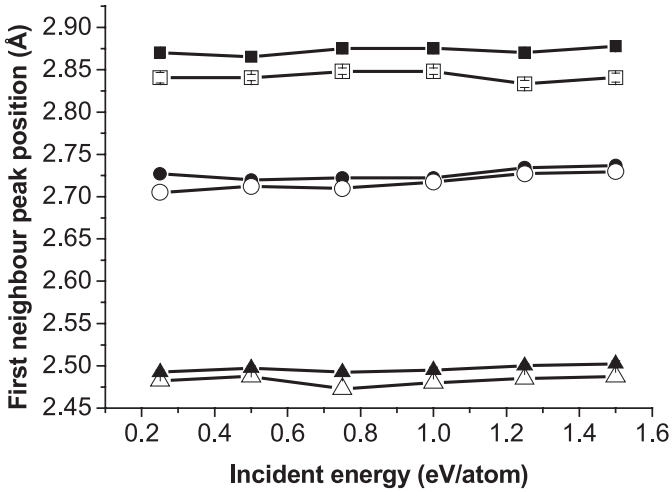

Fig. 8. First neighbour peaks positions as functions of the slowing down energy. The error bars are smaller than the points. Dark squares: small cluster, Ag–Ag peak, open triangles, Co–Co peak in the small cluster, Dark circles: Ag–Co peak in the small cluster, open squares: Ag–Ag peak in the big cluster, dark triangles: Co–Co peak in the big cluster, open circles: Ag–Co peak in the big cluster.

truncated on top. At the highest energies considered however, because of the partial implantation of the clusters, such accommodation with surface rows is more difficult and no polygonal aspect of the interface is observed. As seen in Figure 6, this does not prevent a high degree of epitaxy. The consequences of the larger cluster impact are different. If the energy of incidence is low enough, the Co core and the top part of the Ag surrounding layer are unaffected by the impact. Facets at the cluster surface are thus those before slowing down. The cluster regions close to the surface accommodate partially with the substrate. As noticed above, a step is generally formed surrounding the cluster and its edge displays partial alignments with surface directions. It may be anticipated that thermal surface diffusion may enhance this alignment.

A fifth characteristic is lattice distortions. Lattice distortions in the clusters result, at short range, in changes in atomic separation distance distributions. These are examined by means of pair correlation functions. Such correlation functions for Ag, Co and Ag–Co pairs are shown in Figure 7. They were obtained as time averages over the last 50 ps evolution of the large cluster impacting at 0.25 eV/at. Figure 7 is representative of all cases investigated. The first neighbour peaks are well defined. Their positions, indicated in the figure, can be evaluated as functions of the slowing down energies and the results are given in Figure 8 for all cases considered. These positions are clearly independent of the incident energy and only slightly depend on the cluster size and the amount of Co in it. They are also similar to the positions of the first neighbour peak in the free clusters. Hence, the slowing down and the interaction with the substrate do not modify the mean first neighbour separations significantly. A close analysis of the pair correlation functions indicates that, except for Co–Co pairs, the first neighbour peaks are significantly asymmetrical. This asymmetry is a combined effect of anharmonicity in thermal vibrations and lattice distortions. The numbers in Table 2 illustrates the situation. This table compares full widths at half-maximum, noted w, of the first peak in the correlation functions for Ag–Ag, Co–Co and Ag–Co pairs. It also gives their left and right half widths, noted w_l and w_r respectively, namely toward small and large separations. The results are given for the free $Co_{285}Ag_{301}$ cluster at 300 K, the same cluster after its deposition at 0.25 eV/atom and the same temperature, and after quenching this deposited cluster and the substrate to 0 K. The full widths are the largest for the deposited cluster at 300 K. This corresponds to a situation where the cluster is only partially accommodated to the substrate (see Fig. 6c). w_l is unchanged after deposition, suggesting the thermal contribution to the peak width to be unchanged by the deposition. In all cases,

Table 2. Characteristics of the first peak profile in the three pair correlation functions, measured in the free $Co_{285}Ag_{301}$, after its deposition at 300 K and 0.25 eV/atom and after quenching. The total peak width at half maximum is denoted by w, its left component by w_l and its right component by w_r. They are given in Angströms.

		Ag–Ag	Co–Co	Ag–Co
Free,	w	0.29	0.21	0.32
300 K	w_l	0.11	0.10	0.11
	w_r	0.18	0.11	0.21
Deposited,	w	0.34	0.23	0.33
300 K	w_l	0.13	0.09	0.12
	w_r	0.22	0.13	0.21
Deposited,	w	0.20	0.11	0.20
0 K	w_l	0.05	0.07	0.04
	w_r	0.16	0.04	0.16

w_r is larger than w_l, except for the Co–Co peaks that are close to symmetrical. The peak asymmetry in the free cluster, which is the most pronounced for the Ag–Co pairs, is consistent, in principle, with an anharmonic character of thermal vibrations. If this was true, anharmonicity would also contribute to the peak structure after deposition. Anharmonicity is not sufficient to explain the asymmetry. Indeed, while w_l is quite small at 0 K, w_r is significant, indicating distortion toward large separations. The increase of w_l and w_r from 0 K to 300 K are similar, indicating that the effect of anharmonicity is small. Hence, among the different possible contributions to the first peak structure, lattice distortion appears to be the dominant effect. Finally, comparing the numbers in Table 2 suggests that most of this distortion already occurs in the free cluster, and its enhancement due to the deposition is only limited.

3.2 Individual approach

At the low energies considered, the fate of incident atoms is not expected to drastically depend on their impact point as is the case at kilovolt energies. This was found in the case of the slowing down of Co atoms with 5 to 30 eV kinetic energies on a Ag surface by MD [30] with the same potential as in this study, consistently with experimental findings [22,29]. As clusters are concerned, since they are three dimensional objects, additional degrees of freedom may lead to some sensitivity on the impact location in a complex way. In order to estimate the magnitude of this effect, the penetrated fraction and the number of substrate atoms displaced to add-atom positions were determined cluster by cluster for ten different impacts, using the same incident energy but selecting the initial cluster orientation and location at random. The standard deviation was found equal to 30 percent of the mean for both quantities, indicating, even at energies as low as 0.25 eV per atom, that the final state of a cluster is significantly dependent on the impact conditions. In order to measure the influence of the cluster orientation on the final state, three different cases were compared for the small cluster, namely, slowing down at 1.5 eV/atom with a {111} facet parallel to the substrate surface, with a {100} facet parallel and with no facet but an edge parallel to the surface. In the first case, the penetration is inhibited but the aspect ratio decreases more than average, while the opposite is found in the latter case. Finally, ten impacts were selected at random, but the cluster orientation was kept constant. In this case, the standard deviations of the penetrated fraction and add-atoms numbers are similar to those obtained when orientations are at random. Hence, from these three computer experiments, it is possible to conclude that fluctuations due to impact point and orientation selection are statistically indistinguishable, but that both contribute.

4 Summary

The present study embraces several aspects of cluster modification subsequent to their slowing down. The comparison of these aspects in the case of well-defined different clusters is made and the picture which emerges is as follows: Whatever the cluster size and energy — in the range investigated —, damage is produced in the substrate. Not surprisingly, the amount of damage increases with the slowing down energy. This damage results in the formation of add-atoms at the substrate surface either originating from the cluster or from the substrate. The latter result from the partial penetration of the cluster. They form a step at its periphery, which may be several atomic layers high. The former flow from the cluster surface and dissipate their initial kinetic energy by diffusing toward more distant isolated add-atom sites or small monolayer islands, well-separated from the cluster area. The core-shell structure of a cluster enhances this flow, decreasing this way part of the excess energy associated with the interface between the core and the shell. The impact does not induce dissociation of the Co groups in the cluster, whatever the stoechiometry. As already known from previous work, both experimental and numerical, small clusters accommodate epitaxially with the substrate. This accommodation is however inhibited when the Co core is large enough. Since this one does not dissociate upon impact, it can only accommodate with the substrate by a rigid rotation which turns out to be hardly induced. Therefore, core-shell clusters — depending on the binding energy of the core — may display defects resulting from the competition between epitaxial accommodation and the random core orientation. The lattice in the free clusters is distorted and this distortion is enhanced by the impact. The memory of the initial cluster morphology is partially preserved after the impact of the larger cluster, both as the core and the shell are concerned. No such memory effect was found for the small cluster, which morphology is destroyed by the impact and its reshaping is governed by the epitaxial accommodation. This process is only partial for the larger cluster considered, within the simulation time of 150 ps.

Hence, at the atomic level, the cluster-substrate system displays a complex structure after deposition and the memory of the initial geometrical properties is only partial. This may have consequences relevant to catalysis, magnetic and optical properties and further work is in progress to gather a better insight about the possibilities to monitor the consequences of the cluster-surface interaction.

The two first authors, AD and AR, are grateful to the Federal Science Policy and the Fonds de la Recherche Fondamentale Collective of Belgium respectively, for grants during their stay at the Université Libre de Bruxelles. This work is part of the IAP 5-1 "Quantum Size Effects in Nanostructured Materials" promoted by the Federal Belgian Government.

References

1. A. Henglein, J. Phys. Chem. **83**, 2858 (1979)
2. A. Henglein, P. Mulvaney, T. Linnert, A. Holzwarth, J. Phys. Chem. **96**, 2411 (1992); A. Henglein, P. Mulvaney, A. Holzwarth, T.E. Sosebee, B. Busenges, Phys. Chem. **96**, 754 (1992)

3. A. Henglein, M. Giersig, J. Phys. Chem. **98**, 6931 (1994)
4. K. Torigoe, Y. Nakajima, K. Esumi, J. Phys. Chem. **97**, 8304 (1993)
5. L.M. Liz-Marzan, A.P. Philips, J. Phys. Chem. **99**, 15120 (1995)
6. J.L Rousset, A.M. Cadrot, F.S. Aires, A. Renouprez, P. Mélinon, A. Perez, M. Pellarin, J.L. Vialle, M. Broyer, Surf. Rev. Lett. **3**, 1171 (1996)
7. J.L. Rousset, A. Renouprez, A.M. Cadrot, Phys. Rev. B **58**, 2150 (1998)
8. J.L. Rousset, J.C. Bertolini, P. Miegge, Phys. Rev. B **53**, 4947 (1996)
9. E.E. Zhurkin, M. Hou, J. Phys. Condens. Matter **12**, 6735 (2000)
10. T. Van Hoof, M. Hou, Appl. Surf. Sci. **226**, 94 (2004)
11. T. Van Hoof, M. Hou, Eur. Phys. J. D **29**, 33 (2004)
12. M. Hou, M. El Azzaoui, H. Pattyn, J. Verheyden, G. Koops, G. Zhang, Phys. Rev. B **62**, 5117 (2000)
13. H. Hsieh, R.S. Averback, H. Sellers, C.P. Flunn, Phys. Rev. B **45**, 4417 (1992)
14. M. Hou, Nucl. Instr. Meth. B **135**, 501 (1998)
15. B. Pauwels, G. Van Tendeloo, E.E. Zhurkin, M. Hou, G. Verschoren, L. Theil Kuhn, W. Bouwen, P. Lievens, Phys. Rev. B **63**, 165406-1 (2001)
16. V.S. Kharlamov, E.E. Zhurkin, M. Hou, Nucl. Instr. Meth. B **193**, 538 (2002)
17. L. Bardotti, B. Prével, P. Mélinon, A. Perez, Q. Hou, M. Hou, Phys. Rev. B **62**, 2835 (2000)
18. K.-H. Müller, J. Apll. Phys. **61**, 2516 (1987)
19. H. Haberland, Z. Insepov, M. Moseler, Phys. Rev. B **51**, 11061 (1995)
20. Q. Hou, M. Hou, L. Bardotti, B. Prével, P. Mélinon, A. Perez, Phys. Rev. B **62**, 2825 (2000)
21. M. Hou, V.S. Kharlamov, E.E. Zhurkin, Phys. Rev. B **66**, 195408-1 (2002)
22. J. Dekoster, B. Degroote, H. Pattyn, G. Langouche, A. Vantomme, S. Degroote, Appl. Phys. Lett. **75**, 938 (1999)
23. P. Mélinon, V. Paillard, V. Dupuis, A. Perez, P. Jensen, A. Hoareau, J.P. Perez, J. Tuaillon, M. Broyer, J.L. Vialle, M. Pellarin, B. Baguenard, J. Lerme, Int. J. Mod. Phys. B **139**, 339 (1995)
24. P. Piseri, A. Podestà, E. Barborini, P. Milani, Rev. Sci. Instr. **72**, 2261 (2001)
25. P. Moskovkin, M. Hou, Eur. Phys. J. D **27**, 231 (2003)
26. J. Verheyden, G.L. Zhang, J. Dekoster, A. Vantomme, W. Deweerd, K. Milants, T. Barancira, H. Pattun, J. Phys. D **29**, 1316 (1996)
27. H. Pattyn, J. Verheyden, W. Deweerd, G.E.J. Knoops, G.L. Zhang, M. El Azzaoui, M. Hou, Hyperfine Interact. **120-121**, 291 (1999)
28. J. Verheyden, S. Bukshpan, J. Dekoster, A. Vantomme, W. Deweerd, K. Milants, T. Barancira, G.L. Zhang, H. Pattyn, Europhys. Lett. **37**, 25 (1997)
29. B. Degroote, A. Vantomme, H. Pattyn, K. Vanormelingen, Phys. Rev. B **65**, 195401 (2001)
30. B. Degroote, A. Vantomme, H. Pattyn, K. Vanormelingen, M. Hou, Phys. Rev. B **65**, 195402-1 (2001)
31. W.C. Swope, H.W. Andersen, P.H. Berens, K.R. Wilson, J. Chem. Phys. **76**, 1 (1982)
32. D.J. Oh, R.A. Johnson, J. Mater. Res. **3**, 471 (1988); R.A. Johnson, Phys. Rev. B **39**, 12554 (1989)